Analysis of Delaminated Hybrid Carbon Fiber Composites in MODE-I

[1]Hassan A. Alessa, [2]Steven L. Donaldson
[1, 2]University of Dayton, 300 College Park, Dayton, OH 45469 USA

Abstract
Failure analysis of laminated composite structures has attracted a great deal of interest in recent years due to the increased application of composite materials in a wide range of high-performance structures. Intensive experimental and theoretical studies of failure analysis and prediction are being reviewed. Delamination, the separation of two adjacent plies in composite laminates, represents one of the most critical failure modes in composite laminates. In fact, it is an essential issue in the evaluation of composite laminates for durability and damage tolerance. Thus, broken fibers, delaminated regions, cracks in the matrix material, as well as holes, foreign inclusions and small voids constitute material and structural imperfections that can exist in composite structures. Imperfections have always existed and their effect on the structural response of a system has been very significant in many cases. These imperfections can be classified into two broad categories: initial geometrical imperfections and material or constructional imperfections.
Keywords: Delamination, composite laminates, CZM.

I. Introduction:

Composites were first considered as structural materials a little more than three quarters of a century ago. From that time to now, they have received increasing attention in all aspects of material science, manufacturing technology, and theoretical analysis. The term composite could mean almost anything if taken at face value, since all materials are composites of dissimilar subunits if examined at close enough details. But in modern materials engineering, the term usually refers to a matrix material that is reinforced with fibers. For instance, the term "FRP" which refers to Fiber Reinforced Plastic usually indicates a thermosetting polyester matrix containing glass fibers, and this particular composite has the lion's share of today commercial market. Many composites used today are at the leading edge of materials technology, with performance and costs appropriate to ultra-demanding applications such as space crafts. But heterogeneous materials combining the best aspects of dissimilar constituents have been used by nature for millions of years. Ancient societies, imitating nature, used this approach as well: The book of Exodus speaks of using straw to reinforce mud in brick making, without which the bricks would have almost no strength. Here in Sudan, people from ancient times dated back to Meroe civilization, and up to now used zibala (i.e. animals' dung) mixed with mud as a strong building material. As seen in Table below, which is cited by David Roylance [1], Stephen et al. [2] and Turvey et al. [3], the fibers used in modern composites have strengths and stiffnesses far above those of traditional structural materials. The high strengths of the glass fibers are due to processing that avoids the internal or external textures flaws which normally weaken glass, and the strength and stiffness of polymeric aramid fiber is a consequence of the nearly perfect alignment of the molecular chains with the fiber axis.

Table 1.1 Properties of composite reinforcing fibers.

Material	E (GN/m^2)	σ_b (GN/m^2)	ε_b (%)	ρ (Mg/m^3)	E/ρ (MN.m/kg)	σ_b/ρ (MN.m/kg)
E-glass	72.4	2.4	2.6	2.54	28.5	0.95
S-glass	85.5	4.5	2.0	2.49	34.3	1.8
Aramid	124	3.6	2.3	1.45	86	2.5
Boron	400	3.5	1.0	2.45	163	1.43
H S graphite	253	4.5	1.1	1.80	140	2.5
H M graphite	520	2.4	0.6	1.85	281	1.3

Where E is Young's modulus, σ b is the breaking stress, b ε is the breaking strain, and ρ is the mass density. These materials are not generally usable as fibers alone, and typically they are impregnated by a matrix material that acts to transfer loads to the fibers, and also to protect the fibers from abrasion and environmental attack. The matrix dilutes the properties to some degree, but even so very high specific (weight – adjusted)

ISSN (Print): 2204-0595
ISSN (Online): 2203-1731

properties are available from these materials. Polymers are much more commonly used, with unsaturated styrene – hardened polyesters having the majority of low to medium performance applications and Epoxy or more sophisticated thermosets having the higher end of the market. Thermoplastic matrix composites are increasingly attractive materials, with processing difficulties being perhaps their principal limitation. Recently, composite materials are increasingly used in many mechanical, civil, and aerospace engineering applications due to two desirable features: the first one is their high specific stiffness (i.e. stiffness per unit density) and high specific strength (i.e. strength per unit density), and the second is their properties that can be tailored through variation of the fiber orientation and stacking sequence which gives the designers a wide spectrum of flexibility. The incorporation of high strength, high modulus and low-density filaments in a low strength and a low modulus matrix material is known to result in a structural composite material with a high strength to weight ratio. Thus, the potential of a two-material composite for use in aerospace, under-water, and automotive structures has stimulated considerable research activities in the theoretical prediction of the behavior of these materials. One commonly used composite structure consists of many layers bonded one on top of another to form a high-strength laminated composite plate. Each lamina is fiber reinforced along a single direction, with adjacent layers usually having different filament orientations. For these reasons, composites are continuing to replace other materials used in structures such as conventional materials. In fact, composites are the potential structural materials of the future as their cost continues to decrease due to the continuous improvements in production techniques and the expanding rate of sales.

Structure of Composites 3 There is many situations in engineering where no single material will be suitable to meet a particular design requirement. However, two materials in combination may possess the desired properties and provide a feasible solution to the materials selection problem. A composite can be defined as a material that is composed of two or more distinct phases, usually a reinforced material supported in a compatible matrix, assembled in prescribed amounts to achieve specific physical and chemical properties. In order to classify and characterize composite materials, distinction between the following two types is commonly accepted; see Vernon [4], Jan Stegmann and Erik Lund [5], and David Roylance [1].

1. Fibrous composite materials: Which are composed of high strength fibers embedded in a matrix. The functions of the matrix are to bond the fibers together to protect them from damage, and to transmit the load from one fiber to another.
2. Particulate composite materials: These are composed of particles encased within a tough matrix, e.g. powders or particles in a matrix like ceramics.

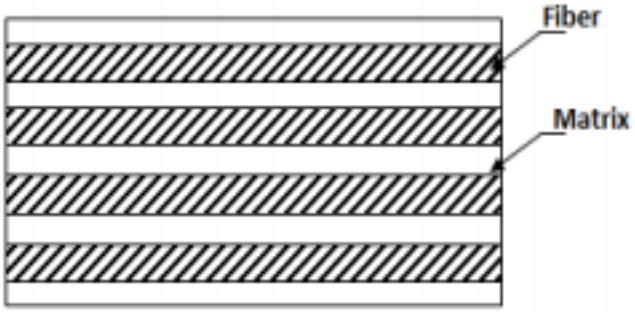

Figure 1.1 Structure of a fibrous composite.

In this study the focus will be on fiber reinforced composite materials, as they are the basic building element of a rectangular laminated plate structure. Typically, such a material consists of stacks of bonded-together layers (i.e. laminas or plies) made from fiber reinforced material. The layers will often be oriented in different directions to provide specific and directed strengths and stiffnesses of the laminate. Thus, the strengths and stiffnesses of the laminated fiber reinforced composite material can be tailored to the specific design requirements of the structural element being built.

Mechanical Properties of Fiber Reinforced Lamina:

Composite materials have many mechanical characteristics, which are different from those of conventional engineering materials such as metals. More precisely, composite materials are often both inhomogeneous and non-isotropic. Therefore, and due to the inherent heterogeneous nature of composite materials, they can be studied from a micromechanical or a macro mechanical point of view. In micromechanics, the behavior of the inhomogeneous lamina is defined in terms of the constituent materials; whereas in macro mechanics the material is presumed homogeneous and the effects of the constituent materials are detected only as averaged apparent macroscopic properties of the composite material. This approach is generally accepted when modeling gross response of composite structures. The micromechanics approach is more convenient for the analysis of the composite material because it studies the volumetric percentages of the constituent materials for the desired lamina stiffnesses and strengths, i.e. the aim of

ISSN (Print): 2204-0595
ISSN (Online): 2203-1731

micromechanics is to determine the moduli of elasticity and strength of a lamina in terms of the moduli of elasticity, and volumetric percentage of the fibers and the matrix. To explain further, both the fibers and the matrix are assumed homogeneous, isotropic and linearly elastic.

II. Literature Review:

Delamination is important phenomenon damage in the laminated composite materials due to weakness of reinforcement through the thickness. The study of the delamination of a laminate may be performed using an approach of fracture mechanics or by introducing appropriate constitutive laws of the interface between the layers constituting the laminate. From a physical point of view, it is reasonable to assume that the second approach can be related to fracture mechanics. In fact, when decohesion occurs between adjacent layers, there is evolution of delaminated surface which is equivalent to the propagation of a crack in a direction a priori known. The literature dealing with the phenomenon of delaminationis very large. A presentation of several structures subjected to the phenomenon of delamination, can be found in [6] and [7]. The delamination phenomenon can be caused by concentration of interlaminar stresses that occur in the vicinity of the free edges or in around of the holes in laminated plates [8]. In addition, the interlaminar defects can grow under a compressive loading. In this case the thin laminated layers degrade (deboning interfaces) and are responsible for increased stresses in the vicinity of the boundaries of delaminated surfaces. In the analysis of the delamination can be distinguished the stage of the crack initiation from the phase of the crack propagation. For prediction of the initiation of a crack from a free edge, the technical Cal culations of the effect of the edge of elasticity [9] and [10], related to criteria based on the average of the normal stresses on a characteristic distance from the edge of the structure [9] are usually used in post- processor of an elastic design in laminated structures. Delamination does not occur necessarily where the stresses are highest. In the phase of the propagation of a delamination established, approaches based on the linear fracture mechanics are generally used. The rate of energy release G is a parameter that is often used to describe the behavior of the phenomenon of delamination in composite materials and structures. G is defined as the energy released from the newly fractured surface and compared to the critical value Gc (This method is used by many authors for the study of crack propagation [10] and [11], but not treat the problem of the initiation of a delamination crack. In contrary the approach of the damage mechanics of the composite can describe the initiation of delamination. The rate of energy release is calculated from the forces and nodal displacements [14] and The state equations and the evolution laws of the interface provided in the context of thermodynamics are described. Models of elastic and damageable interface are presented in [12] and generalized in. In these models, special interface elements are applied in areas where the delamination phenomenon is likely to occur. Elements plane strain with cubic interpolation functions were introduced for discretization of the laminate ply [15]. Other models have been developed for modeling damage layer and interface phenomena [16]. These models are based on the damage mechanics. The interface is considered as a three-dimensional medium with negligible thickness compared to the other dimensions. Therefore, the interface can be considered as two-dimensional entity witch transfers traction and displacement from one layer to the other [17]. The interface is assumed to be dependent on the fiber orientation of adjacent layers and it is assumed to be elastic and damageable. Delamination may be caused by interlaminar stress [18]. The objective of this paper is to present a method to simulate progressive delamination based on a new mixed-mode failure criterion in the context of damage mechanics. This study will highlight the positive contribution of the powder core dates incorporated in the new woven composite. The date cores powder incorporation has an increase effect of the mechanical characteristics giving to the hybrid composite a better behavior and reducing certain types of degradation like delamination. It is important to recognize that, with the advent of composite media, certain new material imperfections can be found in composite structures in addition to the better – known imperfections that one finds in metallic structures. Thus, broken fibers, delaminated regions, cracks in the matrix material, as well as holes, foreign inclusions and small voids constitute material and structural imperfections that can exist in composite structures. Imperfections have always existed and their effect on the structural response of a system has been very significant in many cases. These imperfections can be classified into two broad categories: initial geometrical imperfections and material or constructional imperfections. The first category includes geometrical imperfections in the structural configuration (such as a local out of roundness of a circular cylindrical shell, which makes the cylindrical shell non circular; a small initial curvature in a flat plate or rod, which makes the structure non flat, etc.), as well as imperfections in the loading mechanisms (such as load eccentricities; an axially loaded column is loaded at one end in such a manner that a bending moment exists at that end). The effect of these imperfections on the response of structural systems has been investigated by many researchers and the result of these efforts can be easily found in books, as well as in published papers. The second class of imperfections is equally important, but has not received as much attentions as the first class; especially as far as its effect on the buckling response characteristics is concerned. For metallic materials, one can find several studies which deal with the effect of material imperfections on the fatigue life of the

ISSN (Print): 2204-0595
ISSN (Online): 2203-1731

structural component. Moreover, there exist a number of investigations that deal with the effect of cut – outs and holes on the stress and deformation response of thin plates. Another material imperfection is the rigid inclusion. The effect of rigid inclusions on the stress field of the medium in the neighborhood of the inclusion has received limited attention. The interested reader is referred to the bibliography of Professor Naruoka. There exist two important classes of material and constructional – type imperfections, which are very important in the safe design, especially of aircraft and spacecraft. These classes consist of fatigue cracks or cracks in general and delamination in systems that employ laminates (i.e. fiber – reinforced composites). There is considerable work in the area of stress concentration at crack tips and crack propagation. Very few investigations are cited, herein, for the sake of brevity.

The most common delamination fracture failure type studies have been under mode I loading. Many of people had been done mode I fracture on composite material experimental and simulation. The studies considered to serve as an important back ground to the current work are discussed below. In 1982, Whitney, Browning and Hoogsteden conducted mode I experiments with four different materials (AS-1/3502, AS-4/3502, T300/V3778A, AS-1/ Polysulfone, and Bidirectional Cloth) carbon fiber reinforced polymer. They calculated the critical energy release rate by using four methods (Area method, Beam analysis, Empirical Analysis, and Center Notch) with different initial crack.[11]. In 1989, N. Sela,O. Ishai and L.Banks, investigated how adhesive thickness effect on fracture toughness of carbon fiber reinforced plastic between 0.04mm -1.01mm. They found if increase the thickness of adhesive will increase fracture toughness and the adhesive thickness range between 0.1-0.7mm [22].

In 1997, Julio F. Davalos did experimental and simulation on hybrid material mode I between wood and fiber-reinforced plastic (FRP) and was using contoured specimen for mode I. The fracture toughness of each wood-wood and FRP-FRP higher than FRP-wood hybrid and he used two method the first one Rayleigh-Ritz and Jacobian derivative method (JDM) [26]. In 1999, Shun-Fa Hwang, Bon-Cherng Shen fabricated mode I specimen hybrid material (carbon fiber and fiber glass). The both beams of mode I specimen had two materials fiber glass and carbon fiber with different fiber orientation and specimen hybrid material (carbon fiber and fiber glass) obtained higher interlaminar fracture toughness compare with non-hybrid specimen [28]. In 2012 Mohammadreza Khoshravan, Farhad Asgari Mehrabadi fabricated mode I specimen hybrid material of carbon fiber/aluminum and did fracture toughness tested. They used modified beam theory (MBT) and compliance calibration method (CCM) to calculate mode I fracture toughness. They studied how crack length effect on crack failure and they used FEA to analyses stress distribution on long of specimen and width of specimen [26].In 2013, Soohyun Nam el.al. Fabricated hybrid specimen mode I of aluminum / Polyurethane (PU) adhesive with chopped glass fiber / steel under temperature -150.

III. Materials and Properties:

3.1 Materials:

This research was conducted using composite materials fabricated from S1-HM Unidirectional (UD) fiber glass, EPON Resin 828, EPI-CURE Curing Agent 3223 (Hardener), TORAYCA T300 unidirectional carbon fiber and fluorinated ethylene propylene (FEP) Optically Clear Film made with Teflon.

The fiber glass was donated from AGY-South Carolina. The resin and the hardener were donated from Momentive Specialty Chemicals in Stafford-Texas.

3.1.1 EPON Resin and Curing Agent:

The epoxy system used had two main components; first component is the epoxy resin 828 and the second part is curing agent 3223. These two components were equally important since both reacted and contributed to the final structure and properties. The curing agent 3223 was added 10% by weight to the epoxy resin 828 to cure. [1]

3.1.2 Curing Agent: EPI-CURE 3223:

DIETHYLENETRIAMINE (DETA), N-(2-aminoethyl-1, 2-ethanediamine) is a linear ethyleneamine with two primary and one secondary amine as shown in figure 2. It is a single-component with clear, colorless, and an ammonia-like odor product [4].

DETA is a liquid agent widely used with epoxy resins for fast cures or where room temperature cures are required (Appendix A). Due to exothermic heat of the reaction and the pot life of the catalyzed resin is quite short; this agent is restricted to small casting applications. Although DETA has good properties at room temperature when it is used in curing process (6).

IV. Panel Fabrications and Sample Cutting:

The simulation using Abaq requires material properties data as input to the9 models. The material properties were collected using tensile test ASTM standard D3039 [4] [5] with strain gage MM (CEA-06-250UW-120). The results were used to calculate , and for the glass and carbon composites used.

They were several steps used to fabricate the specimens for the tensile tests. The fabrication lay-up is shown in Figure 3.1. First, the dry fiber plies were cut into pieces with dimension 19” x 18” (482.6 mm x 457.2mm) for fiber glass. The dimensions for dry carbon fiber pieces were 12” x 12” (304.8mm x 304.8mm). The table surface was cleaned by wiping with acetone. Third, the sealing tape was placed (High Temp Sealant Tape-Yellow) with dimensions of 19.25” x 18.25" (488.95mm x 463.55mm) for fiber glass and for carbon fiber sealing tape dimension 12.25” x 12.25” (311.25 mm x 311.25 mm) was used. Fourth, the non-porous Teflon (234 TFNP non-adhesive non-porous) was

ISSN (Print): 2204-0595
ISSN (Online): 2203-1731

placed over the sealing tape to build a dam structure, which kept the resin contained.
The dimension used for the dry fiber glass was 22" x 21" (558.8 mm x 533.4 mm) and for carbon fiber 15" x 15" (381 mm x 381 mm). Fifth, the resin/harder were well mixed 10:1 by weight, then the epoxy was poured on the Teflon (dam structure). The epoxy was then distributed equally by a squeegee. The first piece of fiber was laid up on Teflon (dam structure), then epoxy was poured on the fiber and was distributed equally by a squeegee. These steps were repeated for the next layers of fibers. The [0]T fiber glass piece was laid up with one layer for fiber orientation The [90]s specimens were laid up with two layers having fiber orientation The [45/-45]T were laid up using two layers with fiber orientation. The [05]T carbon fiber pieces were laid up using five layers for fiber orientation . The carbon [904]s were laid up with eight layers having fiber orientation . Finally, the carbon [45/-45]5s was laid up ten layers for fiber orientation. After the fiber was laid up and resin applied, a layer of non-porous Teflon with thickness 0.003" (0.0762 mm) was placed on top, then an aluminum caul plate with thickness 0.118" (3 mm), after that Teflon with thickness 0.003" (0.0762 mm). Following that, the breather layer was then covered by vacuum bagging with vacuum port and seals the vacuum bagging on the edge by sealing tape and leaks were checked. Finally the vacuum pump was connected to vacuum port and turns on the vacuum pump and keeps it running for 24 hours.

The composite panels were then stored for ten days in room temperature to make certain they were fully cured. Then, the composites panels were then cut with dimension 10" (250 mm) over length for unidirectional and symmetric, but were cutting with dimension 7" (175 mm) over length for unidirectional. The tabs were fixed by super glue with 2.25" (56 mm) length and 0.062" (1.5 mm) thickness for unidirectional panel, 1" (25 mm) length and tab thickness for unidirectional panel. The composite panels were cut into tensile specimens with dimension 0.5" (15mm) x 10" (250mm) x 0.04" (1mm) for fiber orientation unidirectional, tensile specimen with dimension 1" (25mm) x 7" (175mm) x 0.08" (2mm) for fiber orientation 9 unidirectional, and tensile specimen with dimension 1" (25mm) x 10" (250mm) x 1" (25mm) for fiber orientation symmetric. They were cut using a wet diamond saw to avoid micro cracks in the specimen.

5. Panel Fabrication and Tests of Mode I:

5.1 Panel Fabrication:

The overall goal of this paper is to discuss the developments of hybrid DCB for mode I,. It will also address the key tasks involved in the development of all three types of composites material such as: (1) Carbon-fiber/Epoxy composite (2) Glass-fiber/Epoxy and (3) Hybrid (Carbon and Glass fibers) composites. The development of a reliable, and, analysis of hybrid DCB, hybrid ENF, and single leg bending (ASLB). The first step in this research was to match bending stiffness of fiber glass and carbon fiber for hybrid DCB, ENF, and ASLB.

Table 5.1 Matched bending stiffness of carbon fiber and fiber glass:

	Thickness m	S1-HM UD TENSILE MODULUS EI	TORAYCA T300 EI	Thickness m
	1.00E-03	50.8	8.466	0.0001
	2.10E-03	106.68	1.69E+01	0.0002
	2.20E-03	111.76	25.4	0.0003
	2.30E-03	1.17E+02	33.866	0.0004
2 layers	2.40E-03	121.92	42.333	0.0005
	2.50E-03	1.27E+02	50.8	0.0006
	2.60E-03	132.08	59.266	0.0007
	2.70E-03	137.16	67.7333	0.0008
	2.80E-03	142.24	76.2	0.0009
	2.90E-03	147.32	84.666	0.001
	3.00E-03	152.4	93.133	0.0011
	3.10E-03	157.48	101.6	0.0012
	3.20E-03	162.56	110.066	0.0013
	3.30E-03	167.64	118.533	0.0014
3.40E-03	172.72	127	0.0015	8 layers
3.50E-03	177.8	135.466	0.0016	

ISSN (Print): 2204-0595
ISSN (Online): 2203-1731

They were several steps necessary to fabricate the tensile test specimens. First, the dry glass fiber plies were cut into pieces with dimensions 19" x 18" (482.6 mm x 457.2mm). The dimension for cutting the dry carbon fiber was 12" x 12" (304.8mm x 304.8mm). Second, the surface of tje table was cleaned from remaining resin or dirt and wiped using acetone. Third, sealing tape with dimensions 19.25" x 18.25" (488.95mm x 463.55mm) for fiber glass, and tape dimension 12.25" x 12.25" (311.25 mm x 311.25 mm) were used for carbon fiber were placed on the tool. Fourth, the non-porous Teflon sheet with dimensions 22" x 21" (558.8 mm x 533.4 mm) for glass fiber and 15" x 15" (381 mm x 381 mm) for carbon fiber was laid up over the sealing tape to build a dam structure to keep the resin contained. Fifth, the resin / hardener were well mixed with 10:1 (by weight) and the epoxy was poured onto the Teflon (dam structure). The epoxy was then distributed equally using a squeegee. The first piece of dry fiber was laid up on the Teflon (dam structure), then epoxy was poured on fiber and was distributed equally by a squeegee. These steps were repeated for the next layers of fibers Fiber Glass Panel The dry glass fiber panels had two distinct sides, as shown in Figures 4.1 and 5.2. The side shown in Figure 5.1 had a small amount of 90° cross weave placed to increase the handing capacity of the primarily unidirectional tows. This face was designated as the 90-face. The opposite face is shown in Figure 5.2.2. It shows the back face of the layer, with the V cross- weaves. This face was designated as the V-face. Therefore, there were three possible combinations of planes for crack growth between glass fiber layers, so the panel fabrication needed to account for this. The first type of fiber glass orientation was denoted as 90/V. Two pieces of fiber glass were laid up with 90 directions facing down Figure 5.2.1. Then, the Teflon insert (0.005") was laid up on top second layer. After that, two more layers were laid up with 90 directions facing down.

The second model of fiber glass orientations called for 90/90 at the center interface. Two wet pieces of fiber glass were laid up with 90 directions facing up and V directions facing down. Then, the Teflon insert 0.0005" (0.0127mm) was laid up on top second layer. After that, two more wet layers were laid up with 90 directions facing up and V direction facing down. The third model of fiber glass orientations called for V/V at the center interface. Two wet pieces of fiber glass were laid up with V directions facing up and 90 directions facing down. Then, the Teflon insert 0.0005" (0.0127mm) was laid up on top second layer. After that, two more wet layers were laid up with V directions facing up and 90 directions facing down.

5.2 Carbon Fiber Panel:

The carbon fiber plies did not have any preferred 'face' or side, They were laid up with ten layers, with distributed epoxy equally on each piece between layers. Then the Teflon insert was laid up on top of the ten layers of carbon fiber. After that, another ten layers of carbon fiber laid up on top Teflon insert.

5.3 Hybrid of Carbon Fiber and Fiber Glass Panel:

They are two types of fiber orientation with the hybrid specimens. The first type of hybrid is referred to as carbon fiber/90 glass fiber. First, two layers of fiber glass with the V direction facing down and 90 facing up were laid down and saturated with resin. The Teflon insert was then laid up on fiber glass 90 faces. After that, ten layers of carbon fiber were laid up.

The second model of hybrid specimens is referred to as carbon fiber/V glass fiber. Two wet layers of fiber glass the 90 directions facing down were laid up, with the V surface facing up. The Teflon insert was then laid up on fiber glass V face. After that, ten wet layers of carbon fiber were laid up.

After the wet fiber plies were laid up, they were covered by a non-porous Teflon 3 mil sheet 3, followed by the aluminum plate, Teflon sheet, breather layer, and vacuum bag. The vacuum bag was connected to a central vacuum port and the vacuum port connected to the vacuum pump. The vacuum pump was run for 24 hours. Following that, each panel was stored for ten days to get full curing. A total of twelve panels were fabricated: three of fiber glass panels, three carbon fiber, and six hybrid panels.

5.4 Sample Cutting:

After ten days (for full cure) the panels were cut into specimens. The fiber glass panel was cut into two pieces for getting Mode I specimens. The Mode I piece has size 8.5" (469.9mm) x 6.25" (158.75mm). The panels edges were parallelized by using a roller sander, as shown in Figure 5.4.4. (5). The carbon fiber and hybrid Figure 5.4.4.(3) panels were also cut into two pieces. Thus we get Mode I pieces for both the carbon and hybrid were 12" (304.8mm) x 5.25" (133.35 mm)], The specimen edges were also parallelized. The dimensions of the Mode I fiber glass specimens were 7" (177.8mm) x 1"(25.4mm). The carbon fiber and hybrid Mode I specimens dimensions were 5" (127mm) x 1"(25.4mm), and 7" (177.8mm) x 1" (25.4)

5.5 DCB Mode I Fracture Static Test:

The Mode I Double Cantilever Beam (DCB) test was developed to measure the interlaminar fracture toughness under peeling stress. The mode I testing conducted in this study was using the unidirectional

ISSN (Print): 2204-0595
ISSN (Online): 2203-1731

fiber (UD) laminates, except with the minor cross-stitch as discussed previously. The fibers directions were along the long axis of the specimens Figure 5.5.2.1.The mode I static testing was conducted following ASTM standard D5528 [8]. Five samples of each of six design were tested to calculate G_{IC}, the mode I interlaminar fracture toughness.

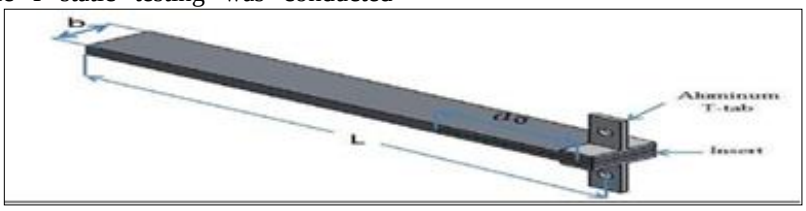

Figure 5.5.2.1. Mode I specimen with T-tab attachment.

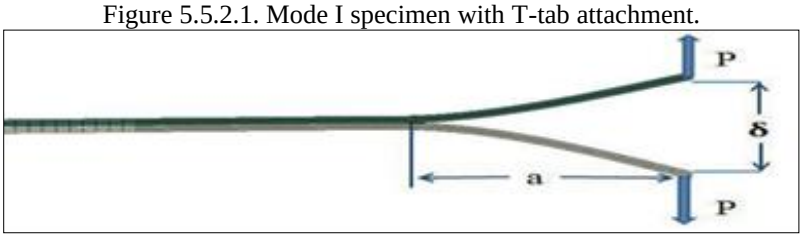

Figure 5.5.2.2 The DCB specimen is in open mode of the static test.

An Instron 5500R Model 1123 was used to provide the mechanical force for the mode I tests. It was a screw-driven mechanical test frame. It was measuring the load, P, and opening distance, Figure 4.5.2.2. The max load of load cell used was 200 lb. The speed displacement rate was 0.1"/min. during the test. A magnifier and bright light source were employed to follow the crack propagation. When the crack propagated and arrived to a mark point, a custom tapping device was used to digitally mark on curve (P vs. δ) to calculate G_{IC}.

In order to conduct the tests, first, each the mode I specimen was attached to the Instron machine by using two pins Figure 4.5.2.3.(1-2). Second, the load and displacement were reset. Note this test did not require mechanically precracking the specimen before the test, because the thin Teflon inserts 0.5 mil was used according ASTM Standard D5528 [8]. Testing was then conducted at a displacement rate 0.1"/minute while the crack propagation was monitored using magnifier and bright light source. The tapping device was taped 10 times, each time when the crack reaches a vertical line during the crack propagation.

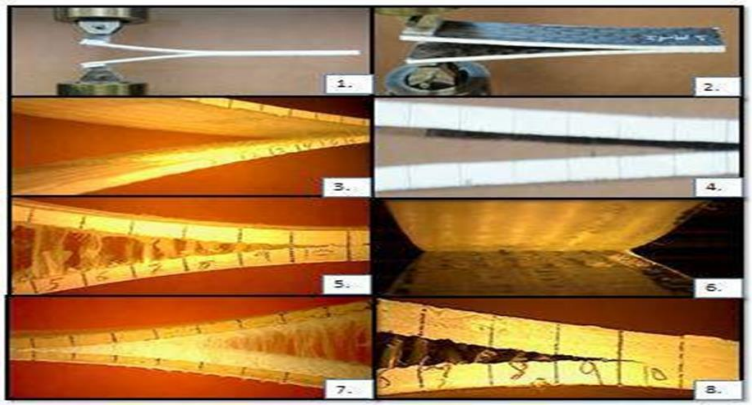

Figure 5.5.2.3 (1-2) Specimen installed in Instron machine by T taps, (2,4)The carbon fiber, (3) fiber glass V-V, (5) fiber glass 90-90, (6) H-CF/FG-V, (7) fiber glass 90-V, (8) H-CF/FG-90.

The FG and CF specimens were attached to the Instron machine by pins in the T-tab as shown in Figure 4.5.2.3 (1-2). The carbon fiber fracture and fiber glass V-V did not show fiber bridging. Figure 4.5.2.3 (3-4). The fiber glass 90-V and fiber glass 90-90 did show fiber bridging. Figures Figure 4.5.2.3 (5) (7). The fracture area of the hybrid H- carbon fiber/ fiber glass V-V did not have fiber bridging, but the carbon fiber side of the specimen appeared to be covered with the fiber of the fiber glass. Figure 4.5.2.3 (6). The hybrid H-carbon fiber/ fiber glass 90 showed fiber bridging Figure 4.5.2.3 (8).

6. Results:

1. Mode I Fracture:

The summary of the Mode I initiation results are shown in Figure 8.24. The pure carbon fiber composite showed the lowest G_{Ic}. This was followed by 90/90 glass fiber, but at approximately double the value. The next higher

ISSN (Print): 2204-0595
ISSN (Online): 2203-1731

results in the all-glass specimens were the V/V specimens; with the highest glass (as well as the highest of all the specimens) were the V/90 specimens. The hybrid specimens, both C-90 and C-V results were similar, and in the range of the all-glass specimens. This is consistent with a visual observation of the fracture surfaces, which showed both faces containing glass. The cracks appeared to propagate in the glass layers of the hybrid specimens.

The summary of the Mode I average results are shown in Figure 8.25. Again, the all- carbon specimen had the lowest value of G_{Ic}. This was followed by all-glass V-V specimen. The all-glass V/90 and 90/90 showed much higher values, which is consistent with the extensive fiber bridging observed. The 90/90 showed the most fiber bridging, which is consistent with the fact that it had the highest G_{Ic} value. The two hybrid designs had results in between the all-glass and all-carbon specimens. Additionally, the C/90 showed more fiber bridging than the C/V, and also a higher average toughness. It should be noted that all of the specimen designs containing 90 had the highest toughness values, which was consistent with the extensive fiber bridging observed in specimens with 90 interfaces.

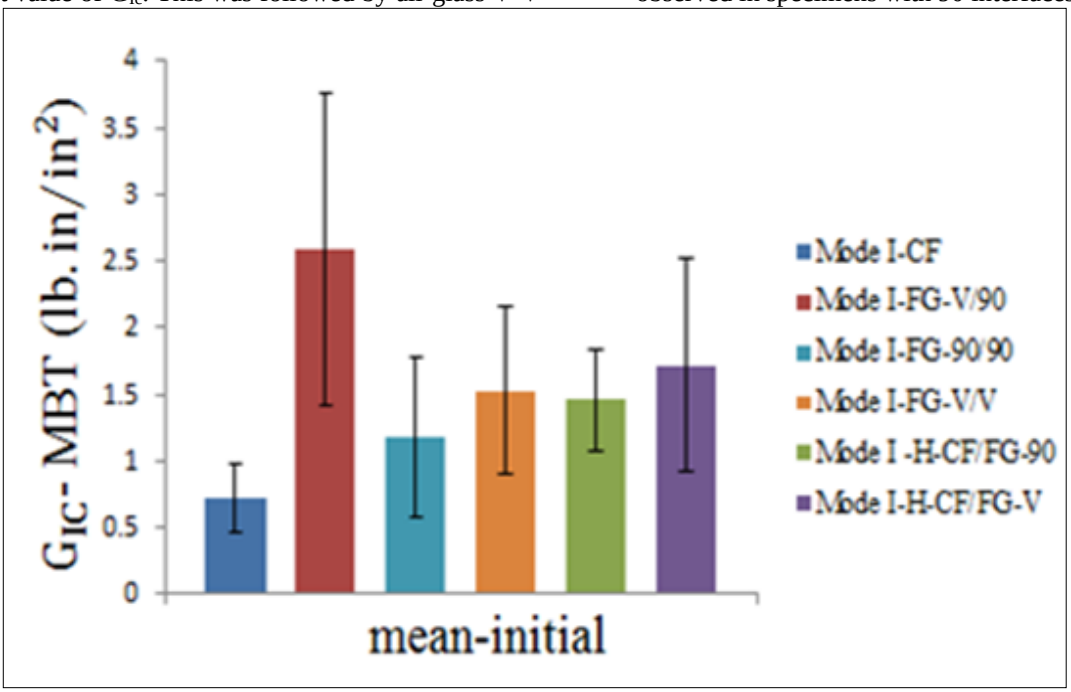

Figure 6.1 Mean initial of mode I strain energy release rate of all mode I specimens by using Modified Beam theory (MBT).

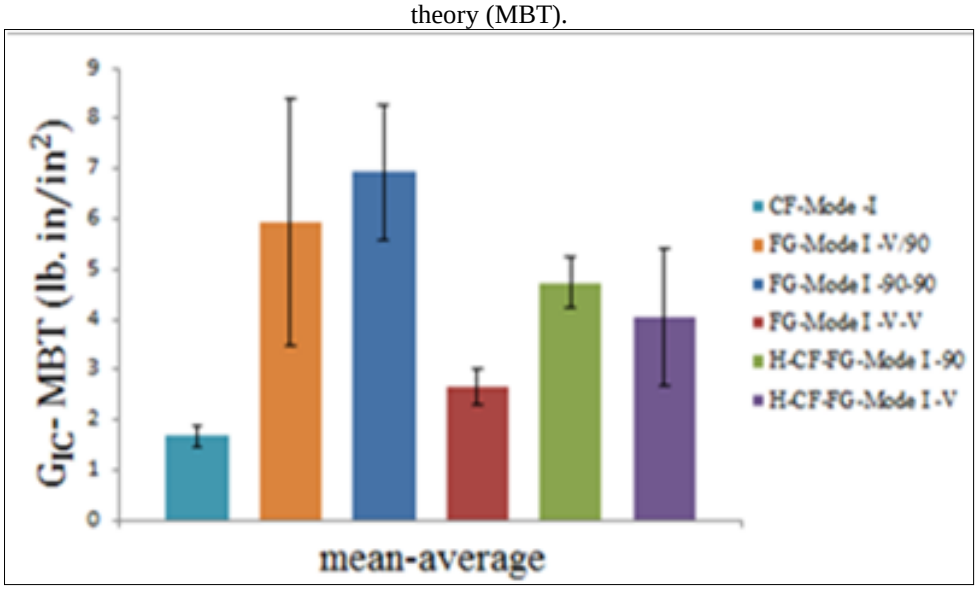

Figure 6.2 Mean average of mode I strain energy release rate of all mode I specimens by using Modified Beam theory (MBT).

6.7.1 Fractographic Analysis:

One of the tools used to assist in understanding the fracture mechanisms is fractographic analysis. In this

ISSN (Print): 2204-0595
ISSN (Online): 2203-1731

study, it was used to interpret fracture behavior of specimens under static mode I, mode II, and mix mode I/II. Each mode has different specimen designs and materials. Each model and design produced unique fracture surfaces. Examples of fracture images were chosen (one of each design and material) from mode I, mode II, mixed-mode I/II.

Mode I Fracture Fractographic:

Figure (6.1 – 6.7) are related to the mode I carbon fiber, fiber glass and hybrid of (FG/CF) sample test of mode I by using scanning electron micrographs (SEM). It helped to compare the fracture surface and interpreting the fracture behavior for each design and mode. The mode I fracture delamination effect by many factors such as fiber bridging, voids, resin rich, regions, and stitches. In all SEM micrographs samples had noticed some common observations. First, all sample did not have resin pockets (the area around Teflon has rich of resin) because it was used Teflon had half mil thickness Second, the crack was propagated between layers of the UD fibers plies.

Figure 6.1 (1-5) is related to the mode I carbon fiber. The crack was propagated between layers of carbon fiber. The mode I carbon fiber had, scarps, fiber tack, voids, river lines, resin-rich and matrix cleavage, but did not had fiber bridging. The specimen had resin-rich, voids around the fiber and that causes the weakness of specimen and crack jumps.

Figures (6.2 – 6.5) are related to the mode I FG (90/V), FG (90/90), and FG (V/V). FG (90/V) had fiber bridging made by 90 fibers plies. It had rich-risen around 90 fibers plies and poor inside the 90 fibers plies. The FG (90/90) had more fiber bridging compare the FG (90/V) and FG (V/V). The crack initiated between 90 fibers plies was making zigzag path because the crack tried find easy way and less resistant. It had scarps around 90 fibers plies. All model of fiber glass had voids between layers of fiber glass, but FG (V/V) had more voids compare with other model of FG specimen. The voids got together around the stitches. The specimen had voids around the fiber and that causes the weakness of specimen and crack jumps and pulling the stitches in reinforcement fiber need more energy so the fracture toughness increased. The FG (V/V) had scarps made by mode I fracture, but did not have fiber bridging and the crack was propagating in the middle of resin between layers.

Figures (6.6 – 6.9) are related to the mode I specimen of H- (FG-90/CF) and H-(FG-V/CF). The specimen of H-(FG-90/CF) had two sides one is FG and other is CF. The side of CF had fiber bridging and fiber tracks cause by 90 fibers glass plies on CF side. It had resin-rich, river shape, voids and scarps cause by fiber glass. The river mark around voids indication to crack initiation from voids [42].The matrix was broken between fibers plies because had gaps between fibers plies Figure 6.6 (2). The FG-90 side had fiber bridging, voids between fibers. It had less fiber bridging less risen compare with CF side. Some area in FG face side has the 90 fibers glass plies and stitches contact with CF face side and the area did not have 90 fibers glass plies did not contact with CF face. The side CF of H-(FG-V/CF) had voids, scarps and some area had bad connected with other surface and the area had fiber glass stitches gave good connected with other surface. The CF side had some fiber stitches from FG side; also the CF surface was more risen compare the FG surface side. The side FG of H-(FG-V/CF) had voids, scarps and some carbon fiber Figure 6.8 (3). That mean the crack propagation change the direction to carbon fiber layer.

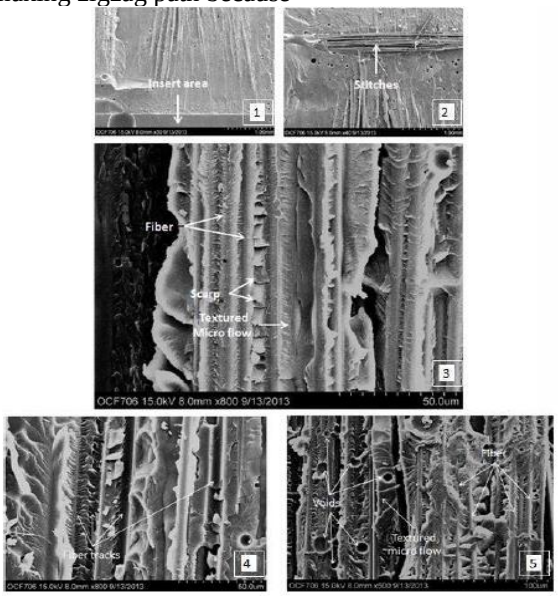

Figure 6.1(1-5) SEM micrographs of carbon fiber specimen fracture surface under static mode I.

ISSN (Print): 2204-0595
ISSN (Online): 2203-1731

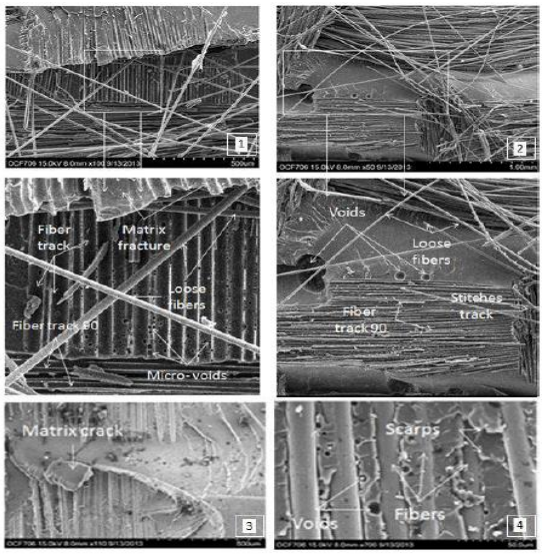

Figure 6.2 (1-4) SEM micrographs of fiber glass (90/V) with V side specimen fracture surface under static mode I.

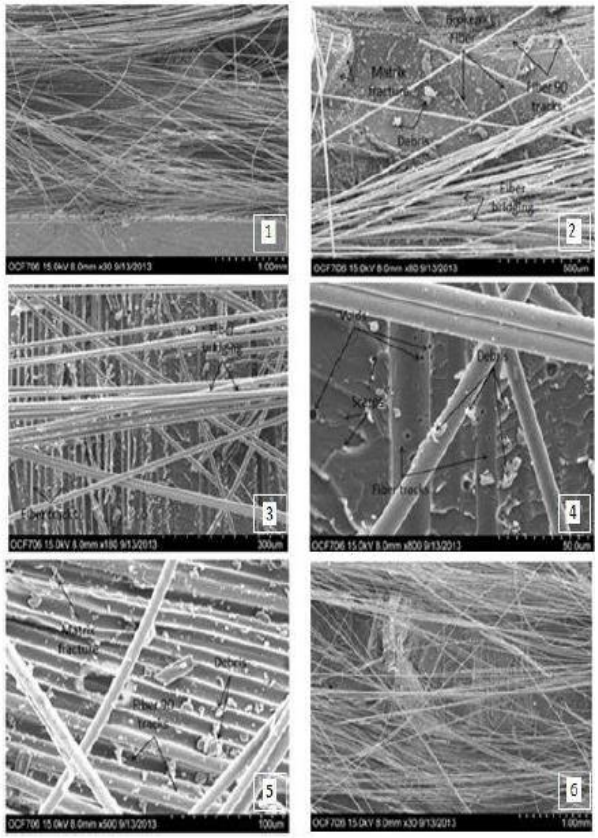

Figure 6.3 (1-6) SEM micrographs of fiber glass (90/V) with 90 side specimen fracture surface under static mode I.

ISSN (Print): 2204-0595
ISSN (Online): 2203-1731

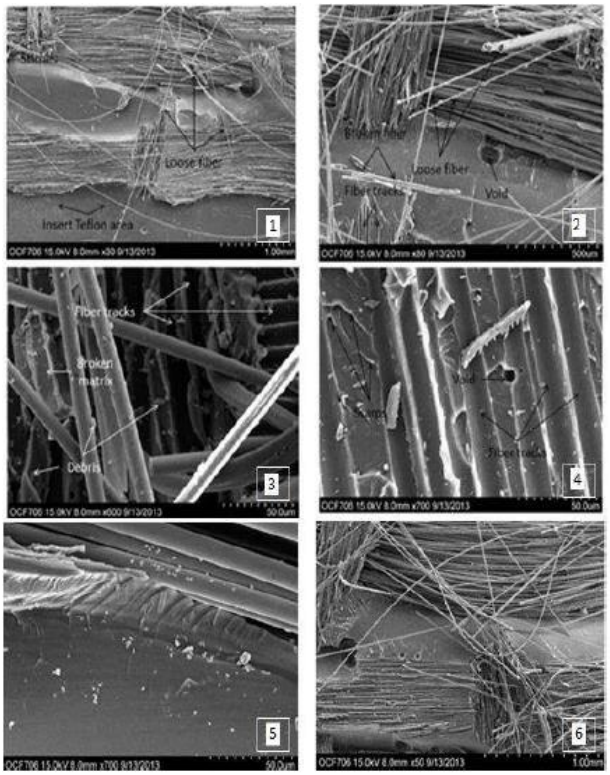

Figure 6.4 (1-6) SEM micrographs of fiber glass (90/90) specimen fracture surface under static mode I.

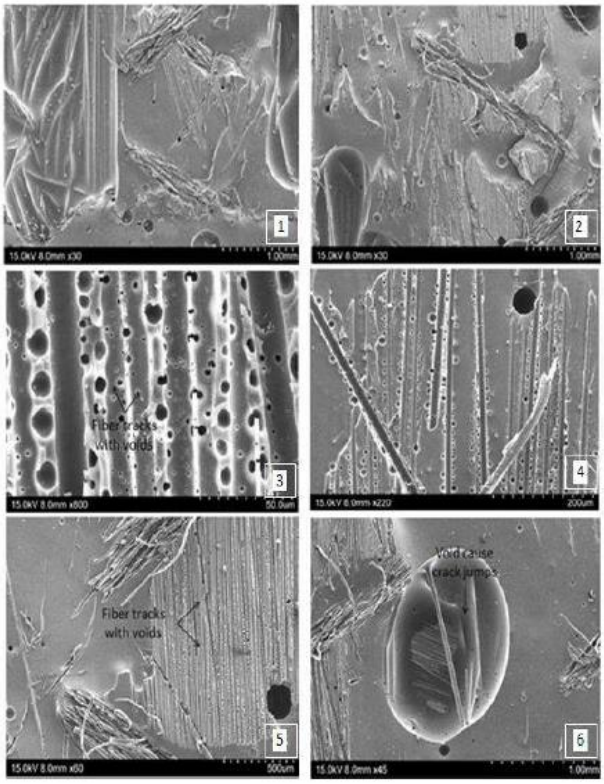

Figure 6.5 (1-6) SEM micrographs of fiber glass (V/V) specimen fracture surface under static mode I.

ISSN (Print): 2204-0595
ISSN (Online): 2203-1731

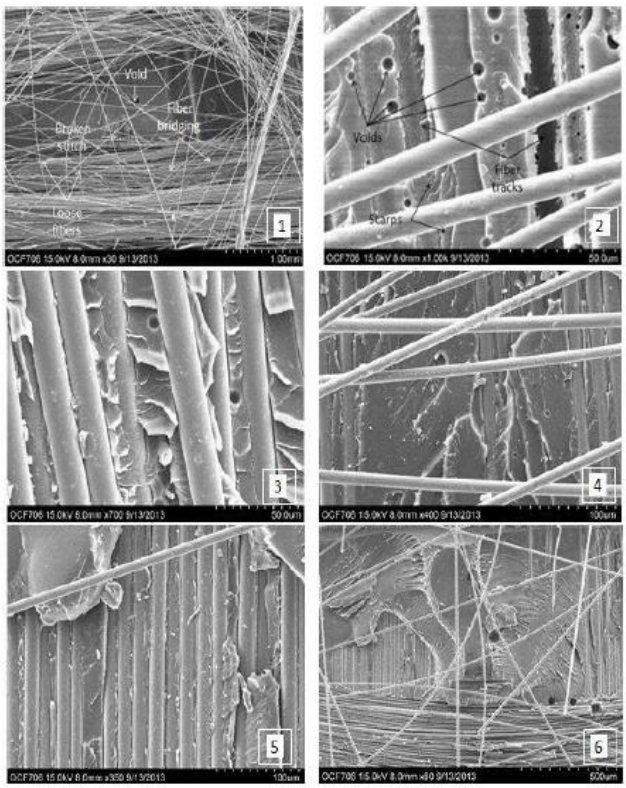

Figure 6.6 (1-6) SEM micrographs of hybrid (FG90/CF) with FG 90 side specimen fracture surface under static mode I.

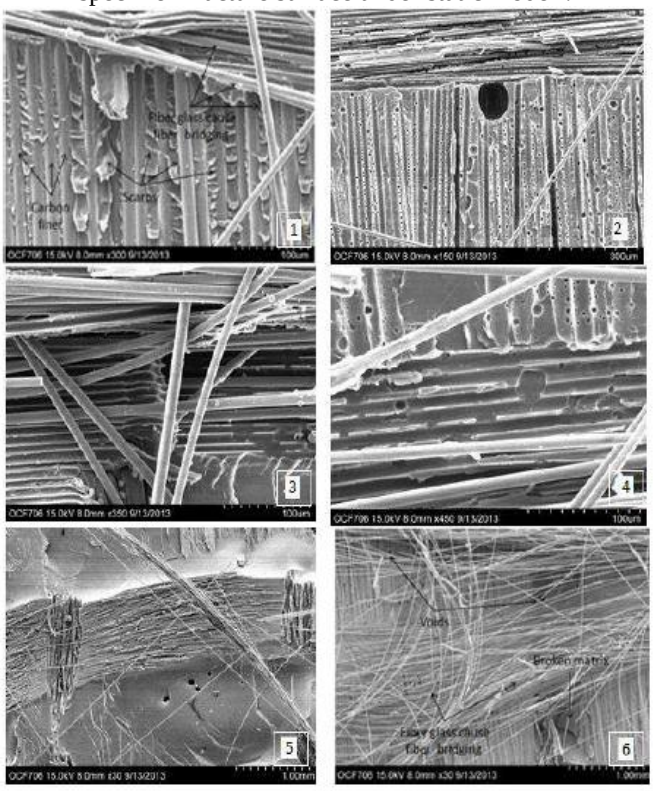

Figure 6.7 (1-6) SEM micrographs of hybrid (FG90/CF) with CF side specimen fracture surface under static mode I.

ISSN (Print): 2204-0595
ISSN (Online): 2203-1731

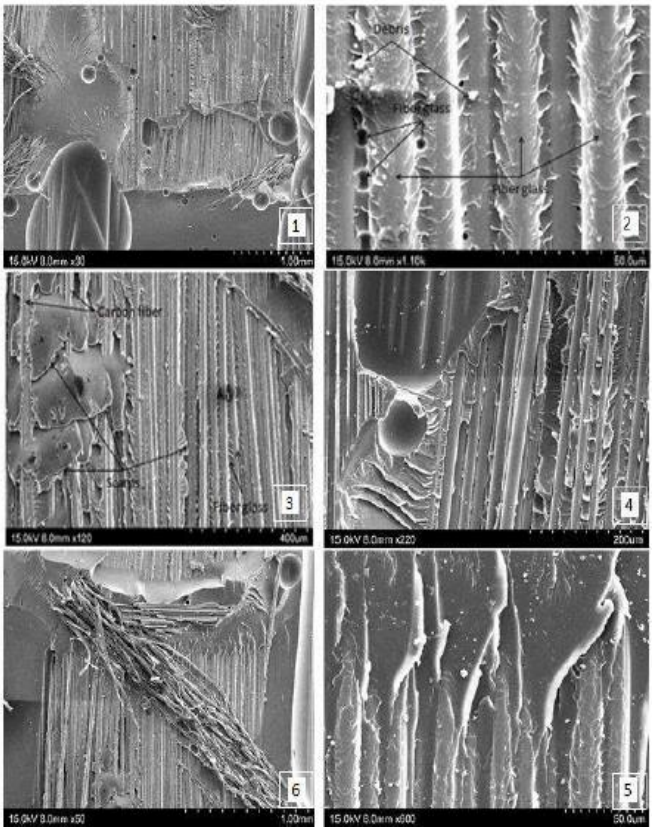

Figure 6.8 (1-6) SEM micrographs of hybrid (FG-V/CF) with FG-V side specimen fracture surface under static mode I.

ISSN (Print): 2204-0595
ISSN (Online): 2203-1731

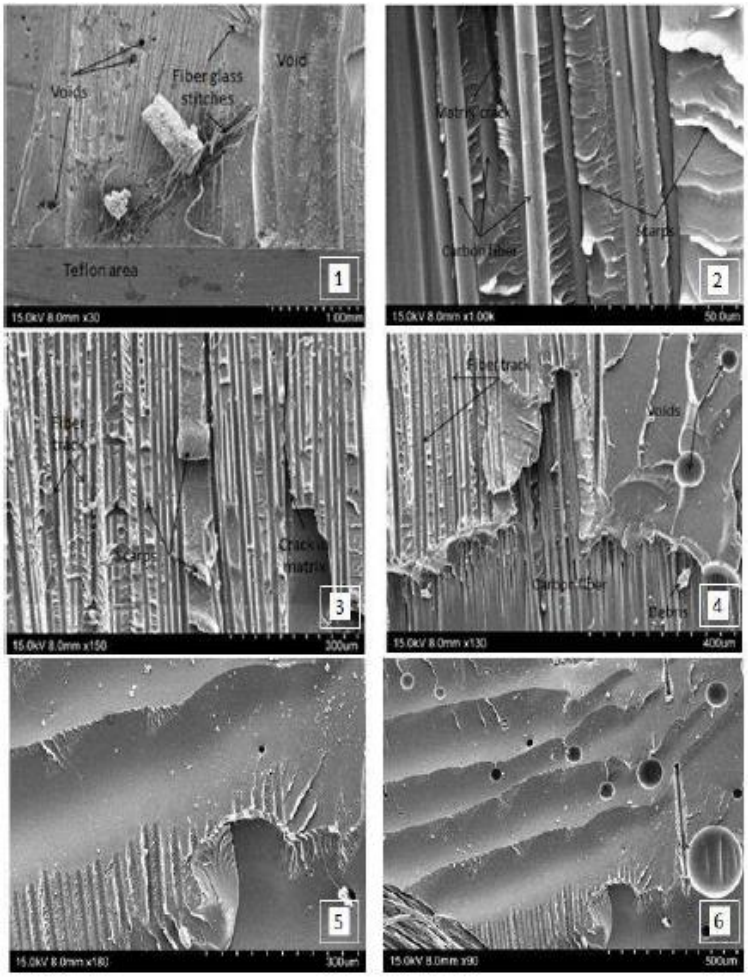

Figure 6.9 (1-6) SEM micrographs of hybrid (FG-V/CF) with CF side specimen fracture surface under static mode I.

Table 8.6.2.3 Fracture toughness for CF mode I:

	1	2	3	4	5	6	7	
	lb./in	lb./in	lb./in	lb./in	lb./in	lb./in	lb./in	N/mm
no.	GI	GI	GI	GI	GI	GI	GI	G-Ave.
1	1.103		0.528	0.579	0.592	1.123	0.703	0.128
2	1.274	0.79	0.837	1.582	0.926	1.51	0.92	0.196
3	1.397	1.264	1.339	1.236	1.096	1.539	1.284	0.229
4	1.897	1.407	1.49	1.646	1.656	2.250	1.336	0.292
5	1.61	1.881	1.993	1.777	1.926	2.287	1.877	0.334
6	1.398	1.833	1.942	2.335	2.118	2.167	1.896	0.342
7	2.178	1.743	1.846	2.532	1.933	2.264	2.094	0.365
8	2.212	1.766	1.871	3.306	1.972	2.48	2.642	0.406
9	2.116	1.890	2.002		2.039	2.394		0.365
10					2.715			0.475
Ave.	1.687	1.453	1.538	1.874	1.697	18.019	12.758	0.313

ISSN (Print): 2204-0595
ISSN (Online): 2203-1731

Table 8.6.2.4 Fracture toughness for mode I FG-90-90

	1	2	3	4	5		
	lb./in	lb./in	lb./in	lb./in	b./in	lb./in	N/mm
no.	GI	GI	GI	GI	GI	G-Ave.	G-Ave
1	1.118	0.848	0.848	1.129		0.986	0.172
2	3.596	3.812	3.812	1.558	6.846	3.925	0.687
3	4.978	5.431	5.431	3.548	6.533	5.184	0.907
4	6.062	6.703	6.703	4.203	7.999	6.334	1.109
5	9.325	8.646	8.646	5.207	8.476	8.06	1.411
6	9.375	10.678	10.678	6.689	6.352	8.754	1.533
7	9.646	10.576	10.576	7.044	5.977	8.764	1.534
8	9.461	10.38	10.389	6.64		7.376	1.614
9	6.362	9.968	9.968	7.289		8.397	1.47
10		10.08	10.08			10.08	1.765
Ave.	6.658	8.57	8.57	4.812	4.687	6.786	1.22

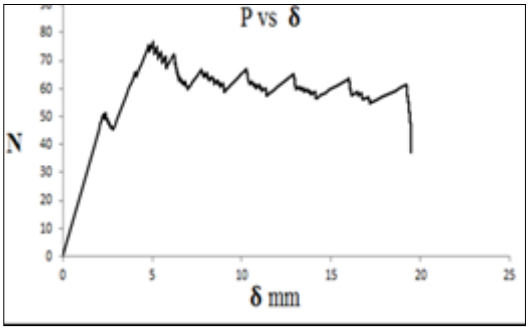

Figure 8.6.5.1 Numerical carbon fiber specimen load vs displacement.

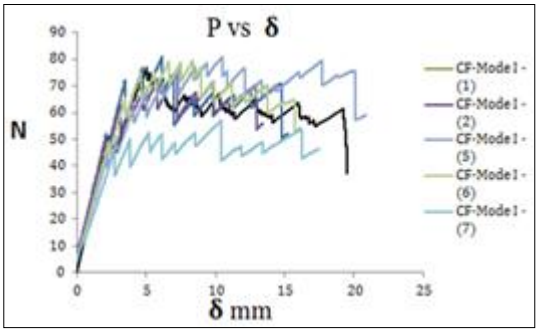

Figure 8.6.5.2 Summary carbon fiber specimen load vs displacement.

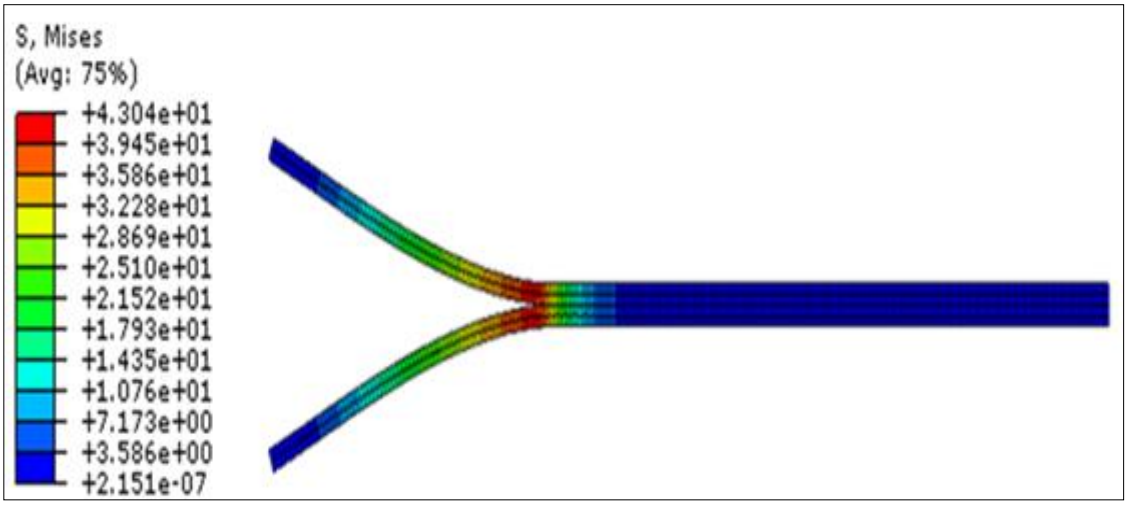

Figure 8.6.5.3 Mises stress of Carbon fiber specimen.

ISSN (Print): 2204-0595
ISSN (Online): 2203-1731

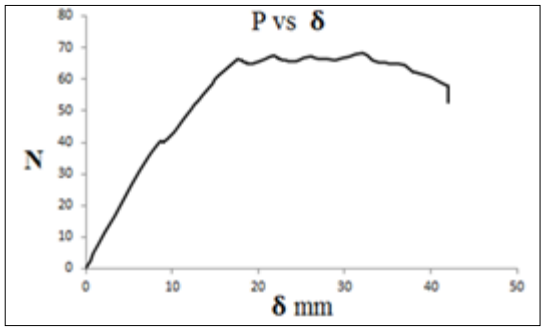

Figure 8.6.6.1 Numerical fiber glass(90/90) specimen load vs displacement.

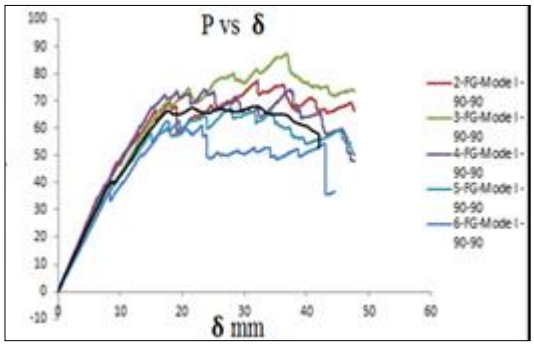

Figure 8.6.6.2Summary fiber glass (90/90) specimen load vs displacement.

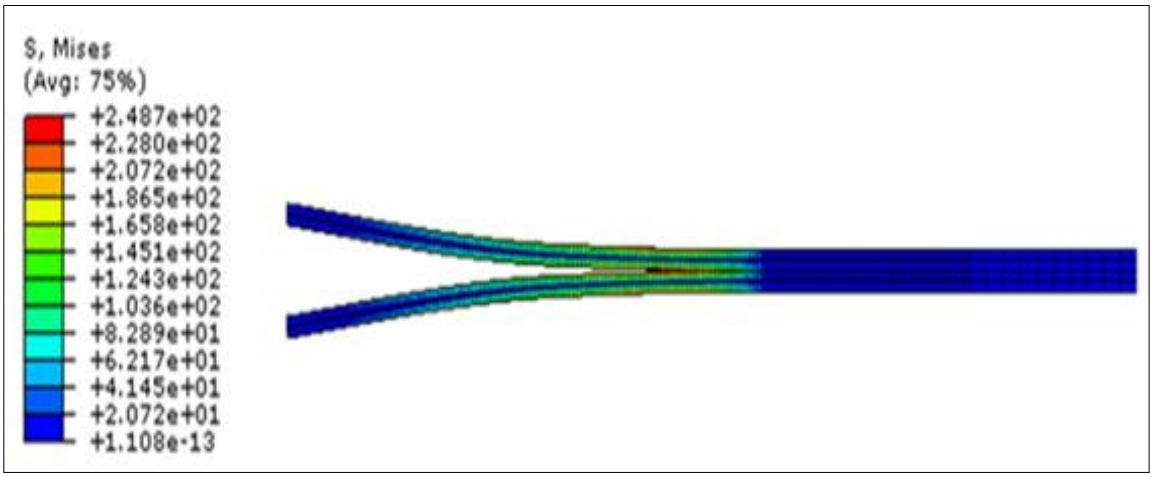

Figure 8.6.6.3 Mises stress of fiber glass (90/90) specimen.

Table 8.6.2.5 Fracture toughness for mode I FG –V/90

	1	2	3	4	5	6		
	lb./in	lb./in	lb./in	lb./in	lb./in	lb./in	lb./in	N/mm
no.	GI	GI	GI	GI	GI	GI	GI-Ave.	GI-Ave.
1	2.558	2.575	2.472	1.857	3.45	5.216	3.021	0.529
2	6.437	2.586	3.737	3.68	6.716	7.415	5.095	0.892
3	7.544	3.096	4.626	3.056	9.483	8.982	6.131	1.073
4	7.918	3.218	5.042	3.25	9.52	9.572	6.42	1.124
5	8.694	2.743	3.819	3.669	11.785	9.313	6.67	1.1682
6	8.237	3.615	3.807	4.08	11.847	8.893	6.747	1.181
7	8.216	3.178	4.601	4.45	11.501	7.726	6.6125	1.158
8	7.424	3.558	4.629	4.448	11.407	7.028	6.416	1.123
9	6.205	4.346	4.622	4.379	8.821	7.073	5.908	1.034
10	5.814	5.39	4.601	5.067	9.443	6.97	6.214	1.088
Ave.	6.905	3.431	4.196	3.793	9.397	7.819	5.923	1.037

ISSN (Print): 2204-0595
ISSN (Online): 2203-1731

Table 8.6.2.6 Fracture toughness for mode I Fiber glass V-V

	1	2	3	4	5		
	lb./in	lb./in	lb./in	lb./in	lb./in	lb./in	N/mm
no.	GI	GI	GI	GI	GI	GI-Ave.	GI-Ave.
1	1.168	2.343	1.123	2.047	0.934	1.523	0.266
2	3.438	5.446	2.102	2.969	0.764	2.944	0.515
3	2.573	2.48	2.417	2.526	1.119	2.223	0.389
4	4.226	2.614	3.054	2.222	2.189	2.861	0.501
5	3.181	1.485	3.412		3.783	2.965	0.519
6	2.981		3.229		2.482	2.897	0.507
7	3.197		2.972		3.694	3.287	0.575
8	3.764		3.571			3.667	0.642
9							
10							
Ave.	3.066	2.873	2.735	2.441	2.138	2.796	3.917

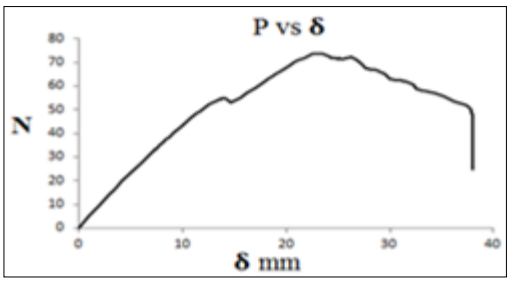

Figure 8.6.6.4 Numerical fiber glass(V/90) specimen load vs displacement.

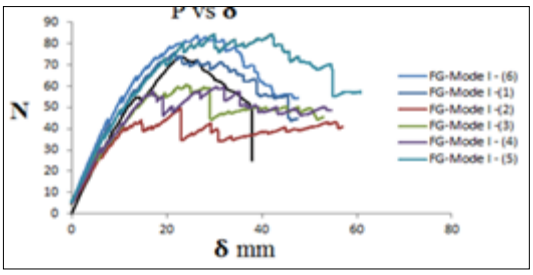

Figure 8.6.6.5 Summary fiber glass(V/90) specimen load vs displacement.

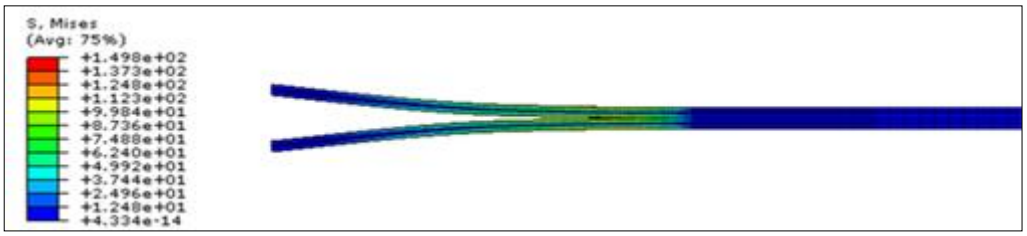

Figure 8.6.6.6Mises stress of fiber glass (V-90) specimen

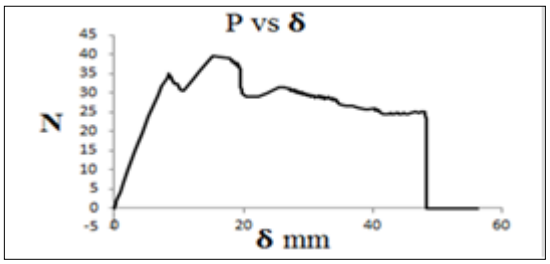

Figure 8.6.6.7 Numerical fiber glass(V/V) specimen load vs displacement.

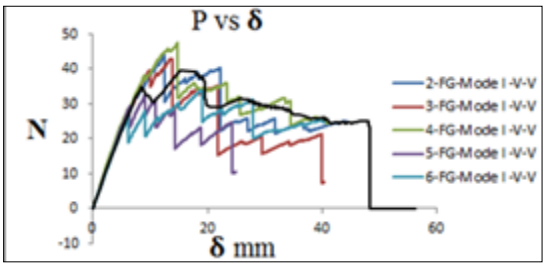

Figure 8.6.6.8 Summary fiber glass (V/V) specimen load vs displacement.

ISSN (Print): 2204-0595
ISSN (Online): 2203-1731

Table 8.6.2.7 Fracture toughness for mode I- H-CF-FG-90

	1	2	3	4	5		
	lb./in	lb./in	lb./in	lb./in	lb./in	lb./in	N/mm
No	GI	GI	GI	GI	GI	GI Ave.	GI-Ave.
1	1.103	1.651	1.527	1.027	1.747	0.705	0.247
2	1.274	3.51	3.344	2.799	3.944	2.479	0.521
3	1.397	3.735	3.794	4.234	3.423	2.764	0.58
4	1.897	4.156	4.832	4.509	4.372	3.294	0.692
5	1.61	4.259	4.822	5.802	5.120	3.602	0.757
6	1.398	4.854	4.964	6.352	4.818	3.7314	0.784
7	2.178	5.019	5.629	5.874	5.912	4.102	0.862
8	2.212	5.162	5.593	6.216	5.74	4.154	0.873
9	2.116	4.867	5.577	5.896	5.135	3.932	0.826
10		4.997	5.523	6.155	4.692	4.273	0.935
Ave.	1.687	4.221	4.561	4.886	4.49	3.304	0.707

Table 8.6.2.8 Fracture toughness for mode I -H-CF-FG-V

	1	2	3	4	5		
	lb./in	lb./in	lb./in	lb./in	lb./in	lb./in	N/mm
No.	GI	GI	GI	GI	GI	GI-Ave.	GI-Ave.
1	1.943		1.869	1.376	1.691	1.376	0.301
2	2.251	3.496	2.469	4.455	9.806	4.495	0.787
3	2.789	5.28	3.097	4.007	5.594	4.154	0.727
4	2.118	6.13	3.908	5.044		4.3	0.753
5	1.993	5.74	2.925	7.125		4.446	0.778
6	2.603	3.07	4.26			3.311	0.579
7	2.358					2.358	0.413
8							
9							
10							
Ave.	2.294	4.743	3.088	4.401	5.697	3.491	0.62

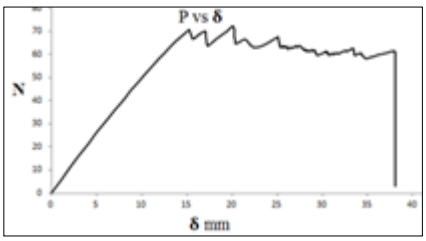

Figure 8.6.6.10 Load vs. displacement of mode I for H-FG (90)/ CF.

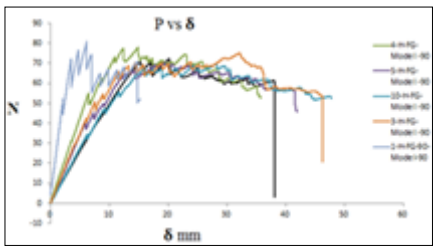

Figure 8.6.6.11Summary of H-FG (90)/ CF specimen load vs displacement.

ISSN (Print): 2204-0595
ISSN (Online): 2203-1731

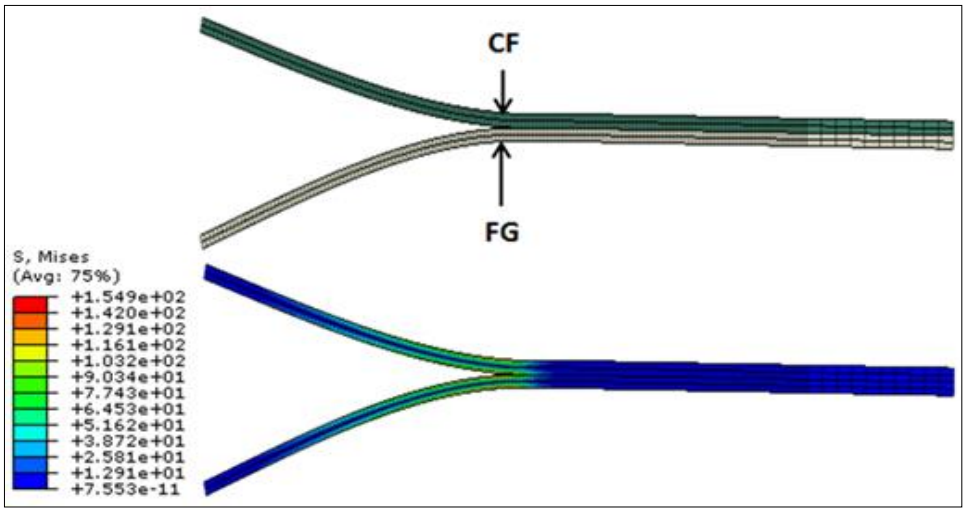

Figure 8.6.6.12Mises stress of hybrid fiber glass (90) and carbon fiber specimen.

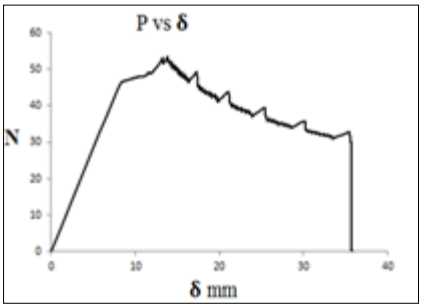

Figure 8.6.6.13Load vs. displacement of mode I for hybrid fiber glass (V) and carbon fiber.

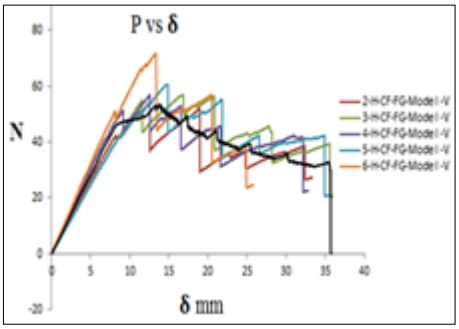

Figure 8.6.6.14 Summary of H-FG (V)/ CF specimen load vs displacement.

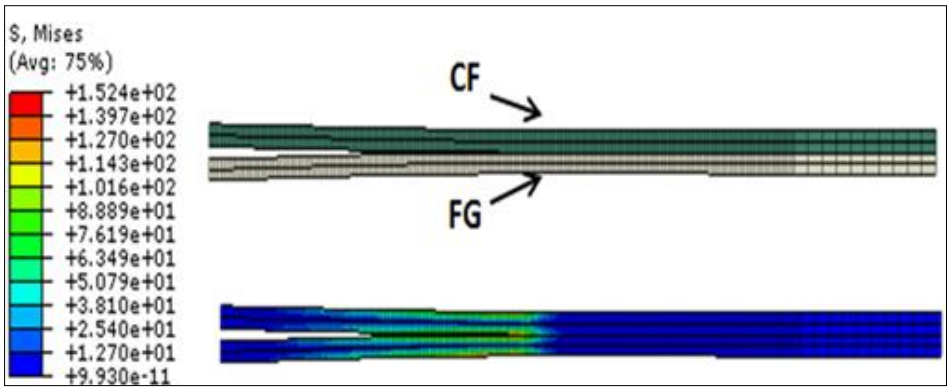

Figure 8.6.6.15 Mises stress of hybrid fiber glass (V) and carbon fiber specimen.

7. Conclusions:

The applications of hybrid composites (such as carbon and glass fiber) materials have been expanding in many fields such as aircraft, wind turbine generators, bridges and infrastructure, sporting goods such as helmets, and marine applications. A composite material may be preferred in applications because of their high strength and stiffness to weight ratio, long fatigue life, and corrosion resistance. In many applications they can be easy to fabricate and offer low cost. The use of hybrid materials offers the ability for designers to balance the high stiffness and strength of carbon fiber, with the high strength and low cost of glass fiber composites. The present study represents of delamination interface of carbon fiber, fiber glass and hybrid-(fiber glass/carbon fiber) under mode I

This study of hybrid interface delamination included:

1. Fabricate S1-HM fiber glass, T-300 carbon fiber and hybrid-(FG/CF) panels using hand lay-up and vacuum bag cure method.
2. Measured the material properties of carbon fiber and fiber glass by tension test specimens. Modulus and Poisson ratios were measured.

ISSN (Print): 2204-0595
ISSN (Online): 2203-1731

3. Mode I Double Cantilever Beam specimens were tested to measure the Mode I interlaminar fracture toughness (energy release rate GIc). The Modified Beam Theory (MBT) was used to calculate energy release rates.

REFERENCES

1. David Roylance, ' an introduction to composite materials', Department of material science and engineering, Massachusetts Institute of Technology, Cambridge; (2000).
2. Stephen W. Tsai, Thomas Hahn H., ' introduction to composite materials', Technomic publishing company; (1980).
3. Turvey G.J., Marshall I.H., 'buckling and post buckling of composite plates', Great Britain, T.J. press Ltd, Padstow, Cornwall; (1995).
4. Vernon B. John, ' introduction to engineering materials', second edition; (1972).
5. Jan Stegmann and Erik Lund, ' notes on structural analysis of composite shell structures', Aalborg University, Denmark; (2001).
6. C. Garg, A damage model in composite structures, Engng. Fracture Mech., 1998. vol. 29.
7. O. O. Ochoa. and ReddyJ.N, Finite elements analysis of composites laminates, Kluwer, 1992.
8. S. Jain and D.C.H. Yang, Effects of federate and chisel edge on delamination in composite drilling. Processing and Manufacturing of Composite Materials, ASME PED 49. 1991. Vol. 27.
9. J.M. Whitney, C.E. Browing and W. Hoogsteden “A Double Cantilever Beam Test for Characterizing Mode I Delamination of Composite Materials” Air Force Wright Aeronautical Laboratories Wright-Patterson, Air Force Base, Ohio 45433, 1982.
10. N. Sela,O. Ishai and L.Banks-Sills ,“The effect of adhesive thickness on interlaminar fracture toughness of interleaved CFRP specimens”,1989.
11. A.J. Brunner, B.R.K. Blackman, P. Davies “A status report on delamination resistance testing of polymer–matrix composites” Science Direct, Engineering Fracture Mechanics, 2007.
12. P.N.B. Reis1a, J.A.M. Ferreira, F.V. Antunes, J.D.M. Costa, C. Capela “Analysis of the initial delamination size on the mode I interlaminar fracture of carbon/epoxy composites”.
13. Mehdi Barikani, Hossein Saidpour, and Mutlu Sezen. “Mode-I Interlaminar Fracture Toughness in Unidirectional Carbon-fibre/Epoxy Composites”.2002.
14. Mohammadreza, Khoshravan, Farhad Asgari Mehrabadi. “Fracture analysis in adhesive composite material/aluminum joints under mode-I loading; experimental and numerical approaches”, International Journal of Adhesion & Adhesives, SciVerse Science Direct,2012
15. Moslem Shahverdi, Anastasios P. Vassilopoulos, Thomas Keller “A phenomenological analysis of Mode I fracture of adhesively-bonded pultruded GFRP joints”,2011
16. Shun-Fa Hwang, Bon-Cherng Shen. “Opening-mode interlaminar fracture toughness of interply hybrid composite materials”.1999.

ISSN (Print): 2204-0595
ISSN (Online): 2203-1731